13th International Symposium on Particle Image Velocimetry – ISPIV 2019
Munich, Germany, July 22-24, 2019

Shake-the-Box PTV in the Wake of an Ahmed Body using Helium Filled Soap Bubbles

Adriaan Booysen, Prashant Das, Sina Ghaemi*

University of Alberta /Department of Mechanical Engineering/Edmonton, Alberta, Canada
*ghaemi@ualberta.ca

Abstract

The Ahmed body was introduced as a simplified model to study the flow field around automotive bodies (Ahmed 1984). Very little is known about the case of crossflow over the square back Ahmed body which can be likened to crosswinds interacting with a transport vehicle. In the present study, we use a combination of an innovative helium filled soap bubble (HFSB) system and time resolved particle tracking velocimetry (4D-PTV) to characterize the flow field in the wake of a square back Ahmed body. The main aim is to investigate the effect of cross-flow (yaw angle, β). The structures of the flow fields were investigated for yaw angles of $\beta = 0°$ and 5°. Analysis of $\beta = 5°$ flow field structure showed the impact of crossflow on the size and shape of the recirculation region. It was found to increase the asymmetry of the recirculation bubble in the spanwise dimension. Lastly three-dimensional proper orthogonal decompositions (POD) of the wakes were carried out and used to identify the dominant structures within the wakes of both the $\beta = 0°$ and $\beta = 5°$ cases. The POD analysis identified the modes contributing to the wake of the square back Ahmed body wake and their corresponding energy levels.

1. Introduction

Society depends on road vehicles as one of the means to ship goods and produce. Large rectangular dimensions are common within the transport vehicle subcategory as they maximize cargo space. However, with this optimization comes aerodynamic sacrifices. Flow around bluff bodies, such as these vehicles, result in significant pressure drag and large separation regions. These shapes are also vulnerable to cross-flow, i.e. a freestream velocity incident to the vehicle at a non-zero yaw angle, β, which can induce stability and handling issues.

The Ahmed body (Ahmed 1984) was introduced as a baseline automotive shape for aerodynamics research. The geometry of an Ahmed body distils the automotive body down to its fundamental aerodynamic shape. Elements of road vehicles such as the rotating tires, side mirrors, complex undertray, and air intakes were eliminated as they only detract from the baseline flow phenomenon. The design was given a blunt nose section, intended to create a large displacement of the flow, a mid-section long enough to allow the flow to reorganize, and a bluff trailing afterbody that formed a well-defined wake. The square back Ahmed body is an iteration of this design that zeros the rear slant seen on initial designs to create a fully rectangular afterbody.

The square back Ahmed body wake at zero yaw has been thoroughly investigated and several primary flow structures have been identified (Grandemange 2013b, Volpe 2015). It was found that the separation at the trailing edge creates a large recirculation region that is symmetric in the spanwise direction and slightly asymmetric along the vertical axis due to the effects of the ground proximity (Grandemange 2013b). The bluff body at zero yaw also has two predominant von Kármán shedding modes corresponding to shedding from the spanwise and vertical edges (Volpe 2015). Lastly, a bistability phenomenon was identified wherein the structure of the recirculation region switches between two stable states in a seemingly random manner (Grandemange 2013b, Volpe 2015).

Research regarding the flow field around a square back Ahmed body with crossflow is sparse. Some studies have looked at the crossflow over bodies similar to the square back Ahmed body; the large eddy simulation (LES) of Hemida (2009) investigates crossflow over a train body, and the partially-averaged Navier-Stokes simulations of Krajnović (2016) characterized the crossflow over a generic vehicle body. Crossflow over the square back Ahmed body has been investigated using 2D particle imaging velocimetry (PIV) measurements to characterize the flow field with yaw angles ranging between $\beta = \pm 6°$ (Bonnavion 2018) and a yaw angle of $\beta = 5°$ (Li 2019). It was determined that the wake starts deviating from the zero-yaw angle case around $\beta = \pm 0.4°$ when the bistability phenomenon is suppressed (Volpe 2015). From the studies investigating the larger yaw angles, it was found that the recirculation bubble shifted towards the windward side of the Ahmed body.

To characterize the spatial organization of turbulent structures, volumetric measurement techniques such as tomographic particle imaging velocimetry (TPIV) (Scarano 2013) and 3D particle tracking velocimetry (3DPTV) (Schanz 2016) are required. Both measurement techniques rely on tracer particles that should accurately follow the flow field and scatter enough light to be detected by the imaging system. These two criteria can be conflicting since tracer fidelity is typically fulfilled by smaller tracers while higher scattered light requires larger particles. The latter limits the size of the measurement domain for volumetric techniques in which high energy density is typically not available through conventional lasers and light-emitting diodes. In addition, a large measurement volume also translates to a large depth-of-field which requires small imaging aperture, further reducing the image intensity. In recent years, a novel method using helium-filled soap bubbles (HFSB) for seeding the flow has proved useful in addressing this challenge (Scarano 2015). These bubbles have a rather large diameter ($\sim$0.5 mm) as compared to the mean diameter of conventionally used fog particles ($\sim$1 μm). This intensifies the scattered light intensity by several orders of magnitude, making it feasible to visualize flow in large volumes.

In an effort to increase the present understanding of the effects of crossflow, we conduct an experimental characterization of the flow field behind a square back Ahmed body. We use a state of the art HFSB system to measure time-resolved volumetric flow using 4D-PTV based on the shake-the-box (STB) algorithm. The obtained measurements are then used to analyse the flow with a non-zero yaw angle case of $\beta = 5°$ and compare it with a baseline case of $\beta = 0°$.

2. Experimental Setup

The crossflow characterization of a square back Ahmed body was carried out in the University of Alberta's closed-loop wind tunnel. The test-section of the wind tunnel has a cross section of 2.4 m × 1.2 m, a contraction ratio of 6.3:1, and a measured turbulence intensity of 0.6%.

A half scale square back Ahmed body was used to characterize the flow field. The body dimensions were 522 mm × 194.5 mm × 144 mm (L×W×H). The body was mounted on a rotary table with a yaw angle precision of $\beta = \pm 0.5°$. A flat plate was positioned underneath and slightly forward of the Ahmed body's leading edge to eliminate the thick turbulent boundary layer forming on the wind tunnel floor and simulate the effects of a roadway. The boundary layer plate was 25 mm below the bottom face of the Ahmed body. The origin of the coordinate system was located on the trailing face of the Ahmed body, centred along the width and height of the Ahmed body rear face at $\beta = 0°$. The x-axis corresponds to the streamwise axis, the y-axis corresponds to the spanwise axis, the z-axis corresponds to the wall-normal axis, and the yaw angle β refers to the counter clockwise rotation of the Ahmed body about the z-axis. All measurements were made at a freestream flow rate of $U_\infty = 10$ m/s corresponding to a Reynolds number (Re_H) of 9.2×10^4. Figure 1 shows the experimental set up used to measure the wake flow field.

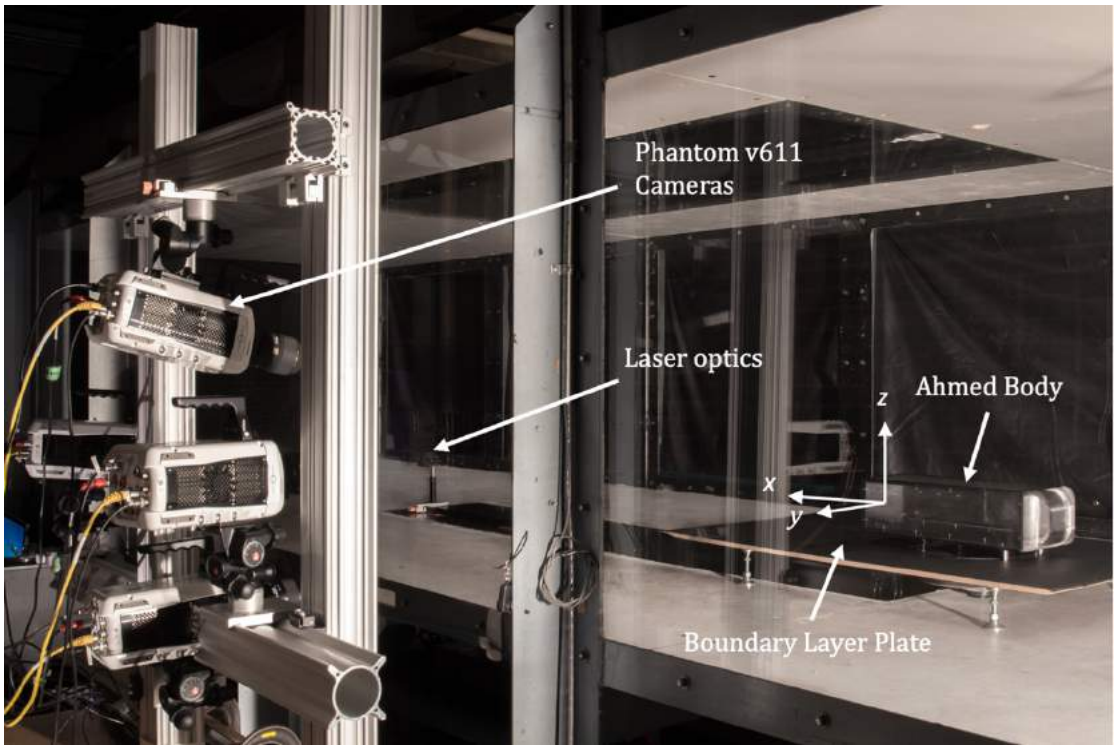

Figure 1: Experimental setup for volumetric measurements of the crossflow over a square back Ahmed body.

The helium filled soap bubble generators were developed at Laboratory of Turbulent flows of the University of Alberta, providing the seeding density needed to carry out the volumetric measurements using 48 nozzles (Gibeau 2018). The seeding system incorporated four ducts mounted

on two support stands with NACA 0012 profiles, to reduce the blockage effects. Each duct supported 16 in-plane nozzles, staggered in both directions to minimize the chances of coalescence between bubbles. Characterizations of the helium filled soap bubbles themselves showed that the bubbles were neutrally buoyant on average with a mean size of 440μm and had a time response of 10 μs with a standard deviation of 148 μs (Gibeau 2019). The HFSB system results in a seeding density of approximately 0.02 particles per pixel.

The imaging system consisted of four Phantom v611 high speed cameras equipped with 105 mm lenses at a working distance of approximately 1.6 m, with apertures of $f/16$, and magnifications of 0.082. The size of the camera sensors was 1280 × 800 pixels. A high frequency 527 nm Photonics Industries dual-cavity Nd: YLF laser with a pulse energy of 20 mJ per cavity was used to illuminate the measurement volume. The laser beam was expanded into the required volume using a -100 mm spherical concave optical lens. The particles were on average 2-3 pixels in size. The measurement volume for the $\beta = 0°$ case measured approximately 350 mm × 240 mm × 180 mm ($x \times y \times z$) and for the $\beta = 5°$ case measured approximately 350 mm × 300 mm × 180 mm ($x \times y \times z$). The measurement volume was located in the wake region of the Ahmed body with a slight overlap of the body itself.

The present work studies two different yaw cases corresponding to $\beta = 0°$ and $\beta = 5°$. For each yaw angle, images were recorded at two different imaging frequencies. The first sequence of images was captured at 2.5 kHz for approximately 2.2 s, resulting in a fully time-resolved data-set. The second sequence involved capturing cycles of 20 time-resolved images at 2.5 kHz, with a cycle frequency of 40Hz. The total duration of measurement using this setting was 25 s. Freestream particle displacement between frames was on the order of 11 pixels. The recorded images were pre-processed using a commercial software (Davis 8.4, LaVision Gmbh). The same software was used to employ the shake-the-box algorithm (Schanz 2016) and generate 3D particle tracks. For each time instant, approximately 5500 tracks were detected. Post-processing of the data was done using MATLAB to evaluate the mean flow field in the wake region. As a first step, particle tracks with a track-length shorter than 7 time-steps were filtered out to remove any potentially erroneous values. Next, the Lagrangian particle tracks were used to generate a Eulerian flow field by fitting a second order-polynomial to individual tracks with a kernel of 7 and then binning the data points in a 3D Cartesian grid. The measurement volume was subdivided into bins with widths of 20 mm in each direction and 75% overlap. Further, proper orthogonal decomposition (POD) of the measured turbulent flow field was carried out to identify the energetic structures of the turbulent flow.

3. Results

The wake for the $\beta = 0°$ and $\beta = 5°$ cases was analysed using 4D-PTV. The first case of $\beta = 0°$ was assessed to provide a baseline for comparison to the crossflow cases as well as provide the means to evaluate the experimental setup and measurement techniques in comparison with the literature. Figures 2a and 2b shows plots of the particle tracks over 20 frames, in the wake region of the Ahmed body, for the $\beta = 0°$ and $\beta = 5°$ cases, respectively.

The figure only shows half of the measurement volume to visualize the recirculation region. The blunt afterbody of the square back Ahmed body creates a large recirculation region which is a defining feature of the $\beta = 0°$ wake, as seen in Figure 2a. Comparing Figures 2a and 2b, for the $\beta = 0°$ case, the

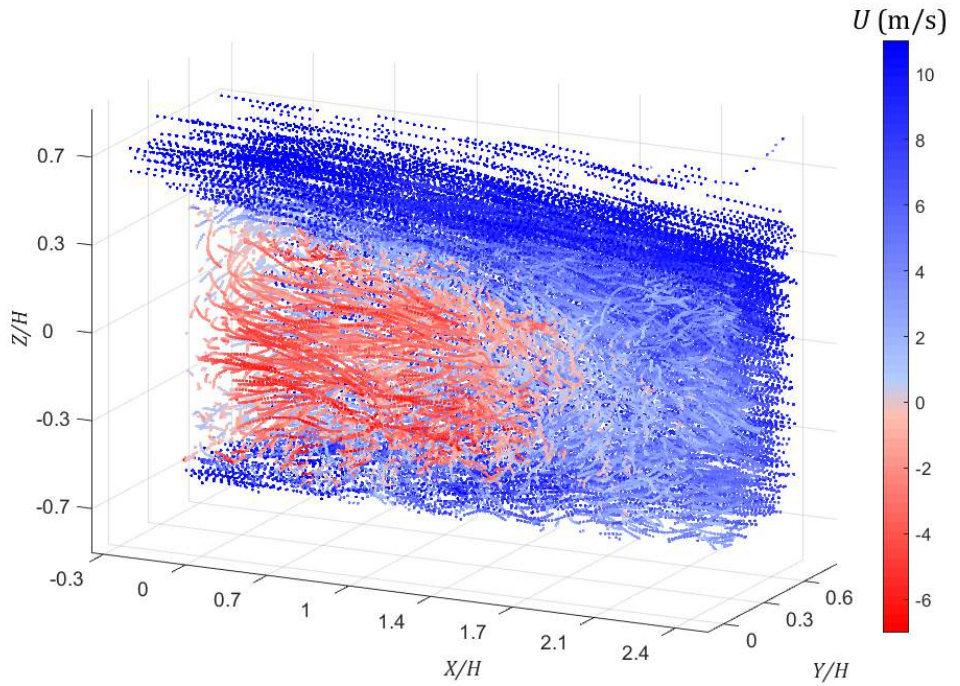

(a)

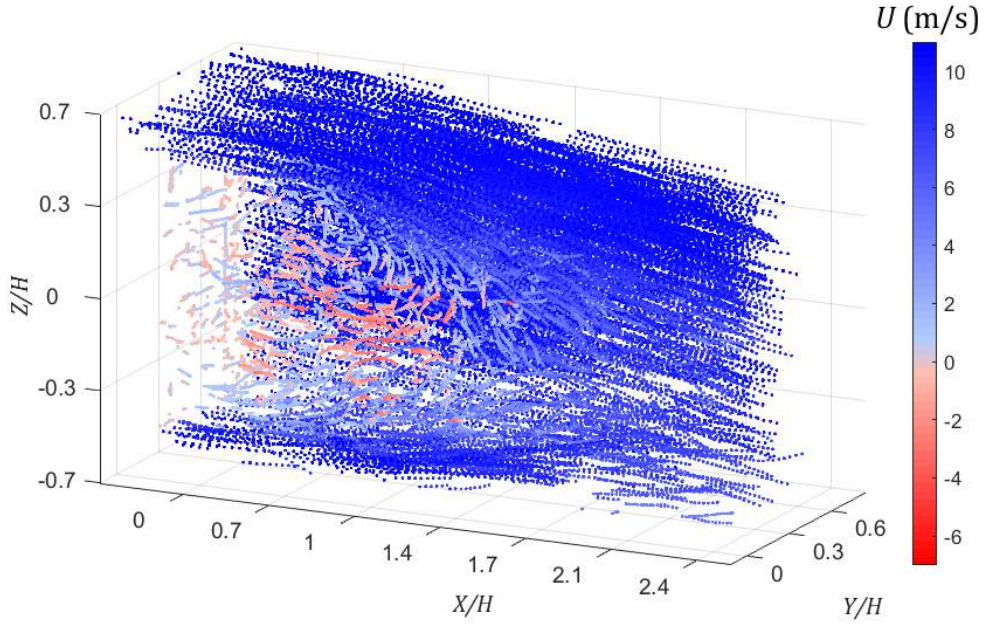

(b)

Figure 2: Instantaneous particle tracks in the wake region for a yaw angle, β, of (a) 0° and (b) 5°. The reconstructed particle tracks shown in each case with a time-step kernel of 15.

magnitude of the reversed flow seen at Y/H=0 appears to be larger when compared to the β = 5° case. The streamwise length of the recirculation bubble, however, remains approximately consistent between cases, as will be shown below.

For a qualitative assessment of the flow structures for both cases; isosurfaces of the mean velocity field at <*U*> = 0 are shown in Figure 3. Figure 3a shows the β = 0° case wherein the recirculation bubble conforms to what has been observed previously (Volpe 2015). The recirculation bubble is almost symmetric across the width and slightly asymmetric along the height of the body due to the ground effect. The length of the bubble is approximately *X/H*=1.55, which is reasonably close to the value of *X/H*=1.47 reported by Grandemange *et al.* (2013b). Figure 3b shows the recirculation region of the β = 5° yaw case. It is seen that the yaw angle affects both the size and shape of the recirculation bubble, increasing the spanwise asymmetry as well as the total width. The streamwise length of the β = 5° recirculation bubble remains approximately the same at *X/H*=1.55.

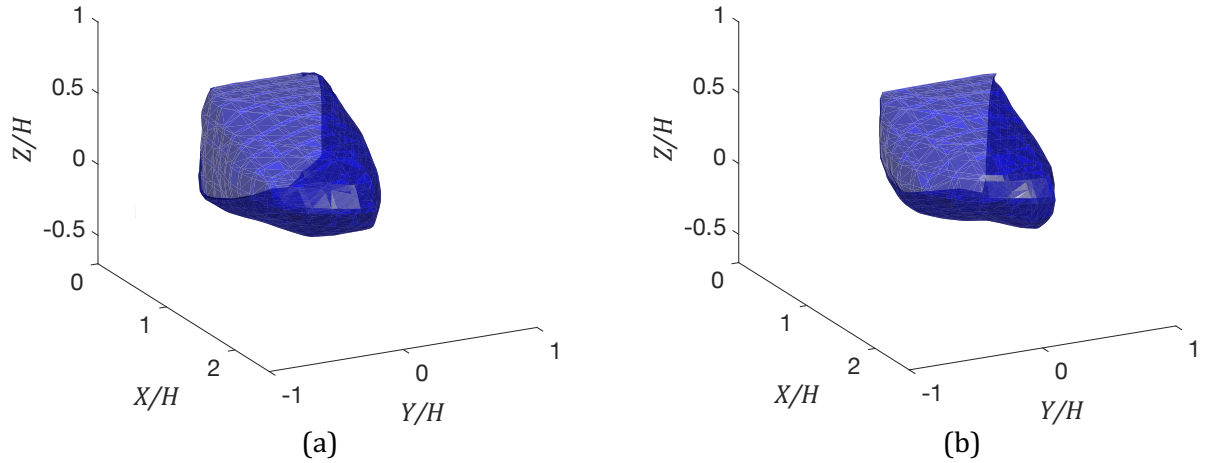

Figure 3: Isosurfaces of the streamwise velocity <*U*>= 0 m/s for a yaw angle, β, of (a) 0° and (b) 5°.

Figure 4 shows the isosurfaces of spanwise velocity at <*V*>= ±1 m/s. Across the two cases in figure 4a and 4b, a notable difference in the size and shape of the isosurface regions can be seen, indicating the changing contributions of the two spanwise velocities to the recirculation region. This demonstrates the added spanwise asymmetry in the flow field. Figure 5 shows the isosurfaces of the wall-normal velocity at <*W*>= ±1 m/s. When comparing the wall-normal velocities between the two yaw angles, differences exist mainly across the spanwise dimension of the domain, again illustrating the increasing spanwise asymmetry of the recirculation bubble.

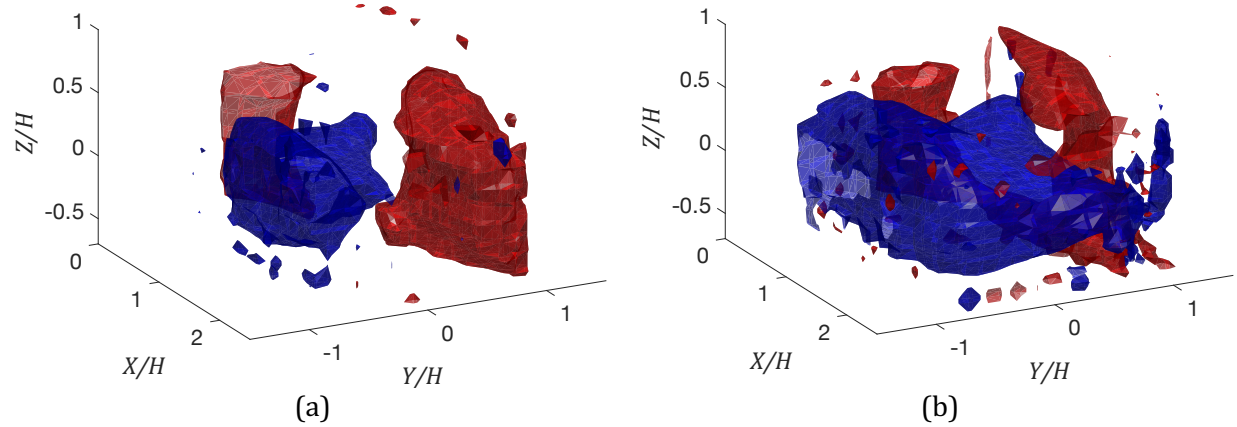

Figure 4: Isosurfaces of the spanwise velocity <*V*>= 1 m/s (blue) and <*V*>= -1 m/s (red) for a yaw angle, β, of (a) 0° and (b) 5°.

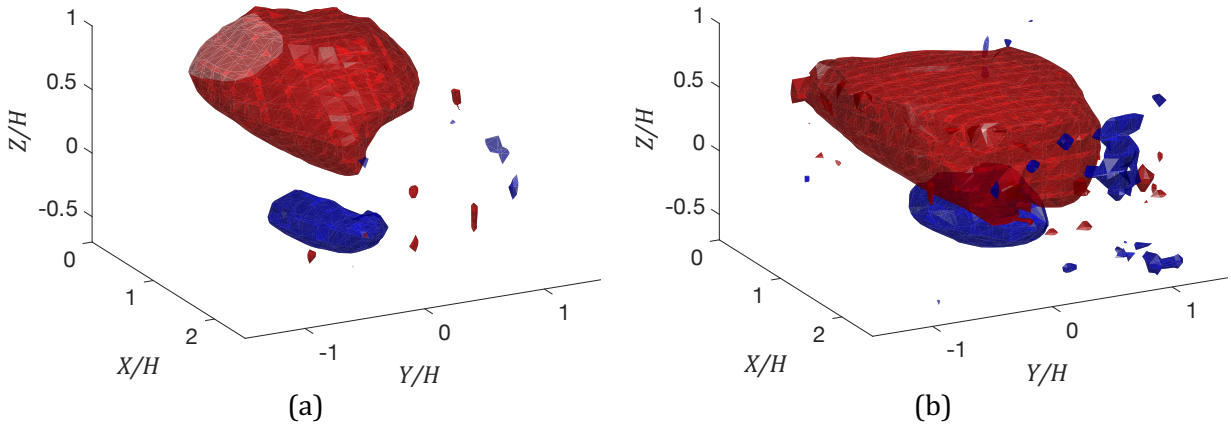

Figure 5: Isosurfaces of the wall-normal velocity <W>= 1 m/s (blue) and <W>= -1 m/s (red) for a yaw angle, β, of (a) 0° and (b) 5°.

Lastly, a POD analysis was completed to identify the energetic modes of the wake flows. Figure 6 shows the first four modes for the β = 0° case. Coherent structures are seen with the first two modes corresponding to spanwise and wall-normal shedding. Figure 7 shows the first four modes of the β = 5° case.

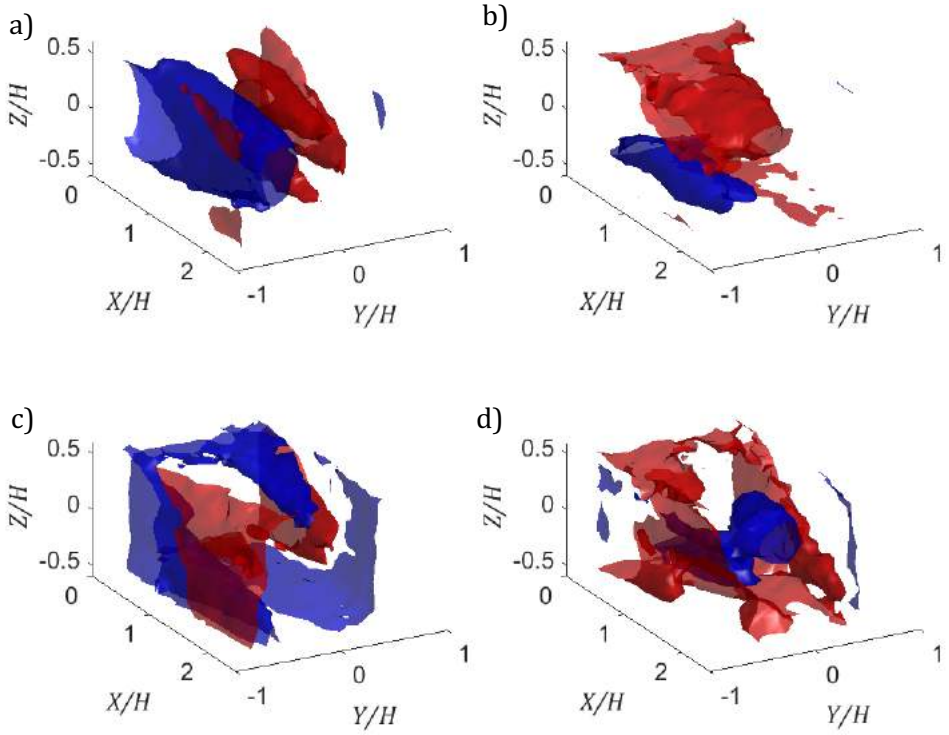

Figure 6: POD modes showing the (a) first, (b) second, (c) third, and (d) fourth most energetic modes for a yaw angle of β = 0°. The isosurfaces represent the normalized mode magnitude at $|\phi|$ = 0.009 for mode 1, $|\phi|$ = 0.01 for mode 2, $|\phi|$ = 0.008 for mode 3, and $|\phi|$ = 0.007 for mode 4. Red isosurfaces represent positive ϕ and blue isosurfaces represent negative ϕ.

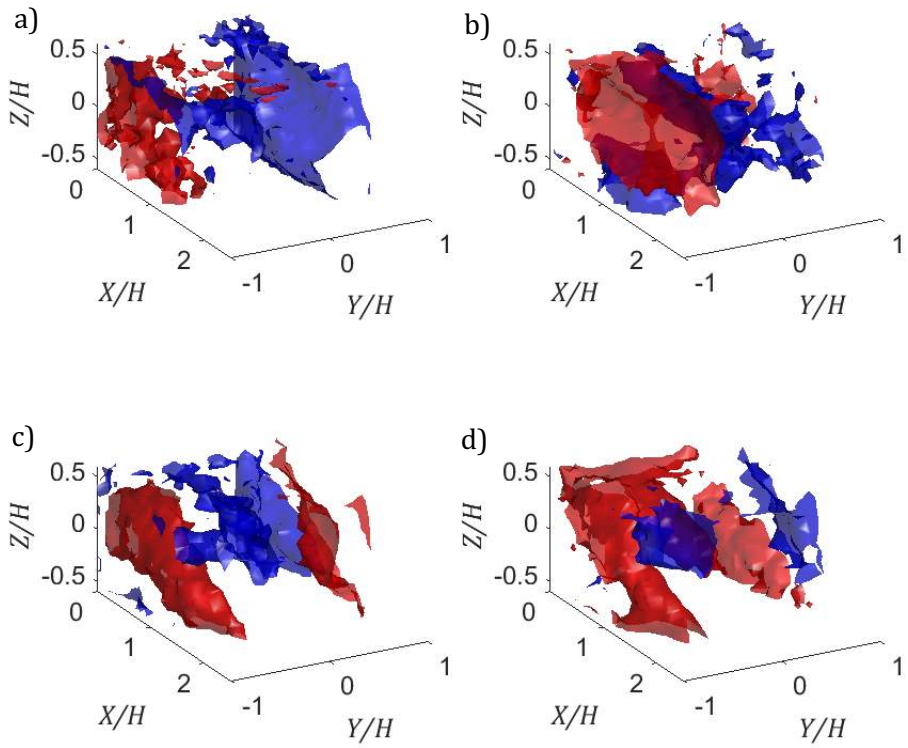

Figure 7: POD modes showing the (a) first, (b) second, (c) third, and (d) fourth most energetic modes for a yaw angle of $\beta = 5°$. The isosurfaces represent the normalized mode magnitude at $|\phi|$ = 0.004 for modes 1-2, $|\phi|$ = 0.007 for mode 3, and $|\phi|$ = 0.008 for mode 4. Red isosurfaces represent positive ϕ and blue isosurfaces represent negative ϕ.

The strength of the modes was assessed by looking at the energy contribution of each individual mode. Figure 8 shows the mode energy distributions for both yaw angles. The first four modes contained 12.2% of the total energy for the $\beta = 0°$ case and 7.5% for the $\beta = 5°$ case. The first mode of the $\beta = 0°$ flow field had the highest energy level of 5.9%. The first mode for the $\beta = 5°$ flow field was 2.3%.

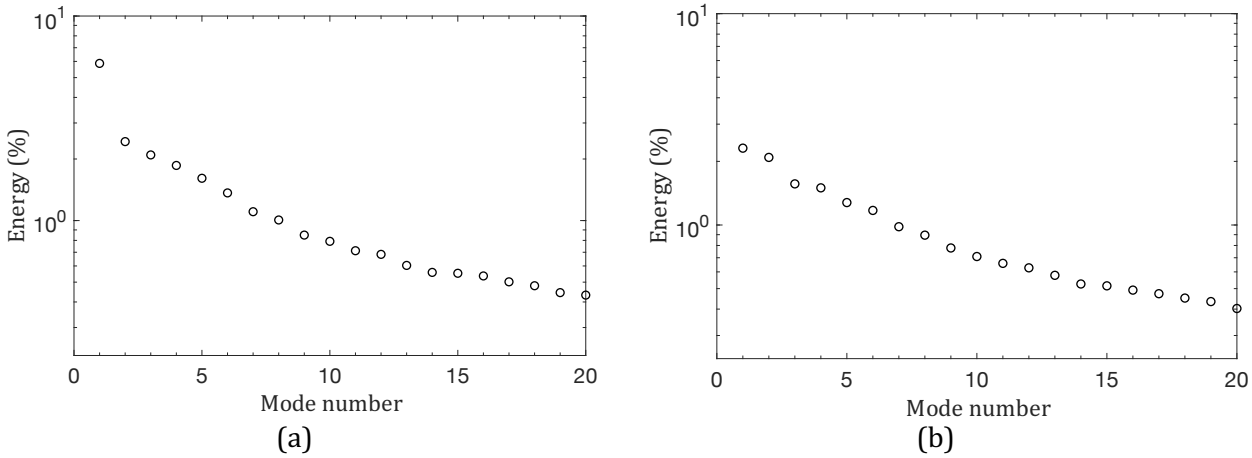

Figure 8: POD mode energy distribution for the first 20 modes. The plots shown are for the yaw angle of (a) $\beta = 0°$ and (b) $\beta = 5°$.

4. Conclusion

In the present study, volumetric flow field measurements were made in the wake of a square back Ahmed body at two different yaw angles of $\beta = 0°$ and $\beta = 5°$. This was achieved using state-of-the-art large-scale HFSB seeding using 48 nozzles and time-resolved 3D particle tracking velocimetry based on the shake-the-box algorithm. The HFSB system produced a seeding density of approximately 0.02 particles per pixel. Using the shake-the-box algorithm, 5500 tracks on average were detected for each instant. The measurement technique allowed for initial preliminary analysis of the wake of the square back Ahmed body at a cross-flow condition as well as a comparison with the baseline. The results for $\beta = 5°$ yaw angle case showed the effects of the crossflow conditions on the asymmetry of the recirculation region. The POD modes for both cases provided insight into which flow structures are dominant within the flow and how much energy they contribute to the overall flow. The first four modes contained 12.2% of the total energy for the $\beta = 0°$ case and 7.5% for the $\beta = 5°$ case. The mode with the largest energy level belonged to the $\beta = 0°$ flow field which contributed 5.9% of the total energy, as compared to the $\beta = 5°$ flow field which contributed 2.3%. With promising results, this 3D measurement presents a solid foundation for further investigation into the crossflow over a square back Ahmed body and the implementation of helium-filled soap bubble seeding systems.

5. References

Ahmed S. R., Ramm G, Faitin G. 1984. "Some salient features of the time - averaged ground vehicle wake." *SAE Technical Paper* 93.

Bonnavion G, Cadot O. 2018. "Unstable wake dynamics of rectangular flat-backed bluff bodies with inclination and ground proximity." *Journal of Fluid Mechanics* 854: 196-232. doi:https://doi.org/10.1017/jfm.2018.630.

F, Scarano. 2013. "Tomographic PIV: principles and practice." *Measurement Science and Technology* 24 (1).

Gibeau B, Ghaemi S. 2018. "A modular, 3D-printed helium-filled soap bubble generator for large-scale volumetric flow measurements." *Experiments in Fluids* https://doi.org/10.1007/s00348-018-2634-9: 59:178.

Gibeau B, Gingras D, Raffel J, Raffel M, Ghaemi S. 2019. "Effect of internal geometry and orientation on the performance of a helium-filled soap bubble nozzle." *13th International Symposium on Particle Image Velocimetry - ISPIV 2019.*

Grandemange M, Gohlke M, Cadot O. 2013a. "Bi-stability in the turbulent wake past parallelepiped bodies with various aspect ratios and wall effects." *Physics of Fluids* (American Institute of Physics) 25 (9): 095103. doi:https://doi.org/10.1063/1.4820372.

Grandemange M, Gohlke M, Cadot O,. 2013b. "Turbulent wake past a three-dimensional blunt body. Part 1. Global modes and bi-stability." *Journal of Fluid Mechanics* 722: 51-84. doi:https://doi.org/10.1017/jfm.2013.83.

Hemida H, Krajnović S. 2010. "LES study of the influence of nose shape and yaw angles on flow structures around trains." *Journal fo Wind Engineering and Industrial Aerodynamics* 98 (1): 34-46.

Krajnović S, Minelli G, Basara B. 2016. "Partially-Averaged Navier-Stokes Simulations of Flows Around Generic Vehicle at Yaw." *SAE Technical Paper* (SAE International) 2016-01-1586. doi:https://doi.org/10.4271/2016-01-1586.

Li R, Borée J, Noack B, Cordier L, Harambat F. 2019. "Drag reduction mechanisms of a car model at moderate yaw by bi-frequency forcing." *Physical Review Fluids* 4 (3): 034604. doi:10.1103/PhysRevFluids.4.034604.

Scarano F, Ghaemi S, Caridi GCA, Bosbach J, Dierksheide U, Sciacchitano A. 2015. "On the use of helium-filled soap bubbles for large-scale tomographic PIV in wind tunnel experiments." *Experiments in Fluids* 56:42. doi:https://doi.org/10.1007/s00348-015-1909-7.

Schanz D, Gesemann S, Schröder A. 2016. "Shake-The-Box: Lagrangian particle tracking at high particle image densities." *Experiments in Fluids* 57:70. doi:https://doi.org/10.1007/s00348-016-2157-1.

Volpe R, Devinant P, Kourta A. 2015. "Experimental characterization of the unsteady natural wake of the full-scale square back Ahmed body: flow bi-stability and spectral analysis." *Experiments in Fluids* (Springer) 56:99. doi: https://doi.org/10.1007/s00348-015-1972-0.